



# ANALYSIS OF FAULTS ON SVC COMPENSATED THREE TERMINAL TRANSMISSION SYSTEM USING WAVELET FUZZY APPROACH

J.Uday Bhaskar,  
Assoc. Professor, Dept. of EEE,  
DMSSVH College of Engineering,  
Machilipatnam, AP, India

G.Ravi Kumar  
Professor, Dept. of EEE,  
KITS, Warangal,  
A.P, India

S.S.Tulasiram  
Professor, Dept. of EEE  
University College of Engineering,  
JNTUH-Hyderabad, Telangana

S.Ramya Lakshmi  
M.Tech Scholar, Dept. of EEE,  
DMSSVH College of Engineering  
Machilipatnam, AP, India

**Abstract**— The increase in the capital expenditure has led to the development of multi terminal transmission system where more than two terminals are interconnected to the system. Faults in a three-terminal transmission system are a major concern in power transmission and distribution. Quick action must be taken to detect and locate these faults so that proper action can be taken to restore the system. The transient stability of a transmission system can be improved by incorporating FACTS devices like SVC which is mainly used for voltage regulation and can rapidly supply dynamic vars required during faults for voltage support. Protection of such interconnected systems is difficult as compared with two-terminal systems. The proposed paper presents the simulation results for the protection of three terminal transmission system compensated with SVC. The fault indices of all the phases for all the faults at each terminal were obtained through MATLAB simulation using wavelet transform with Bior1.5 as mother wavelet. The fault indices were utilized to detect and classify the faults and also to identify the faulty terminal with variations in fault impedance and fault inception angle which are independent of each other. The fault location has been estimated with Fuzzy Inference System(FIS). The proposed protection scheme was found to be fast, reliable for detection of various types of faults at all terminals with variations in fault location and fault inception angle.

**Keywords**— Three terminal transmission, Wavelet transform, Fault index, SVC, Threshold value, Fault inception angle, Fuzzy Inference System

## I. INTRODUCTION

The compensation of a three terminal transmission system with FACTS devices like SVC improves the transient stability

and rapidly supplies dynamic vars required during faults for voltage support in transmission and distribution systems where the reactive power injected or absorbed by SVC influences the apparent impedance in over reaching or under reaching of distance relays. The application of FACTS devices in power systems emphasizes the capability of controlling network conditions and improving voltage stability. SVC is connected in shunt with the transmission system which gives maximum benefits in terms of stabilized voltage support and power transfer capability. The increases in the capital expenditure and obtaining the right-of-way have led to the development of multi terminal transmission system where more than two terminals are interconnected.. Power transfer in most multi terminal transmission systems is constrained by voltage and power stability which will limit the utilization of transmission networks. Protection of such interconnected systems is complicated as compared with two-terminal systems, since these lines will have the problems of in feed currents from the other terminals or an out feed to the terminals. Changes in the section lengths and source impedances, superimposing of currents lead to the system protection under fault conditions. There are a number of protection schemes for multi-terminal transmission circuits such as unit and non-unit schemes. Bo,Z.Q, proposed a unit scheme, which require extensive communication channels between the line ends[1]. Bhalija, B., and Maheswari,R.P proposed an adaptive distance relaying scheme to detect high resistance faults on two terminal parallel transmission line[2]. Brahma et al proposed a fault location scheme for a multi-terminal transmission line based on synchronized voltage measurements at all terminals [3]. Lyonette, D.R.M et al proposed a different directional comparison techniques for multi-terminal lines, which compare the polarity of fault generated transient current signals [4]. B.Bhalija et al proposed a differential protection scheme for tapped transmission lines where out feed current in case of internal



and external faults was considered [5]. Al-Fakhri proposed differential protection scheme for multi-terminal lines with incremental currents [6]. Funabashi et al utilized synchronized current inputs from all terminals and developed two different methods to locate the fault[7]. Prarthana Warlyani et al used voltage and current signals of each section of teed circuit to detect and classify L-L-G faults and the detection was in one cycle.[8]. Peyman Jafarian et al proposed a method based on high frequency transients generated by faults to cover the total length of multi terminal transmission lines[9]. A.H.Osman, O.P Malik proposed a wavelet transform approach to distance protection of transmission lines, an application of wavelet transform to distance protection of transmission lines.[10]. The technique is based on decomposing the voltage and current signals at the relay location using wavelet filter banks. K.Saravanababu et al utilized DWT for fault detection and location estimation[11]. Atthapol Ngaoppitakkal et al, identified the simultaneous faults in transmission line using DWT and Fuzzy logic algorithm.[12]. Chul-Hwan Kim et al proposed in their paper novel fault-detection techniques of high impedance arcing faults (HIF) in transmission lines using the wavelet transforms[13]. The technique is based on using the absolute sum value of coefficients in multiresolution signal decomposition (MSD) based on the discrete wavelet transform (DWT). A fault indicator and fault criteria were then used to detect the HIF in the transmission line. In order to discriminate between HIF and non-fault transient phenomena It was shown that the technique developed was robust to fault type, fault inception angle, fault resistance and fault location. M.Kowsalya et al emphasized the optimal positioning of svc along the transmission line[14],where it was located at the middle of the transmission system for enhanced power transfer capability. F.A.Albasri et al emphasized the impact of shunt facts devices on distance protection of transmission lines[15],where the impact of SVC on the performance of transmission lines and the application it is used for and also the location in the transmission system were given. Rekha et al presented the reactive power control of transmission line with firing angle control of SVC [16]. S.A.Hosseini et al presented new method for identifying transmission line faults with high impedance[17]. Fengliang et al applied wavelet transform and emphasized the performance of digital filters for effective operation of the relays for distance protection[18].Ravikumar et al proposed the double transmission line protection in the presence of svc with wavelet approach[19]. There must be some innovative methods to be developed for three terminal transmission line protection .In this paper, wavelet multi-resolution analysis has been used for detection and classification of faults on three-terminal transmission circuit compensated with SVC. Detail D1 coefficients of current signals at all the three phases and at all the terminals were used to detect and classify the faults. The current signals were analyzed taking into consideration that sum of the current coefficients at all the three terminals.

## II. WAVELET ANALYSIS

Wavelet Transform (WT) is an effective tool for analysis of transient currents and voltages, analyses the signal in both frequency and time domains, by using short and long windows for high and low frequencies respectively. This helps to analyze the signal in both the domains effectively. A set of basis functions called wavelets, which are obtained by mother wavelet to decompose the signal in different frequency bands called approximates and details. The amplitude and incidence of each frequency band can be found precisely. Wavelet Transform (WT) is defined as a sequence of functions  $\{h(n)\}$  (low pass filter) and  $\{g(n)\}$  (high pass filter).  $\phi(t)$ ,  $\Psi(t)$  can be defined by the following equations.

$$\phi(t) = \sqrt{2} \sum h(n)\phi(2t - n), \psi(t) = \sqrt{2} \sum g(n)\phi(2t - n)$$

Where  $g(n) = (-1)^n h(1-n)$ .

This theory gives vital information related to the frequency and time domain decomposition of a waveform through different levels of resolution. The feature extraction property of Wavelets Transforms is exploited in protection of transmission lines for detection and classification of the faults. The different types of wavelets include Haar, Daubechies, Symlet, Bior etc. and the selection of mother wavelet is based on the type of application and system configuration; since Bior-1.5 has been found to be effective and chosen as mother wavelet.

## III. PROPOSED SYSTEM

Figure 1 shows the single line diagram of the three terminal transmission system considered along with the various blocks of the proposed scheme. Three 110-km, 400 kV transmission lines compensated with Static Var compensator (SVC) at each terminal are interconnected. A 300-Mvar Static Var Compensator(SVC) regulates voltage on a 6,000-MVA, 400-kV system.The SVC consists of a 400 kV/16-kV 333-MVA coupling transformer, one 109-Mvar Thyristor Controlled Reactor Bank (TCR) and 94-Mvar Thyristor Switched Capacitor banks (TSC1 TSC2 TSC3)of three number are connected on the secondary side of the transformer.

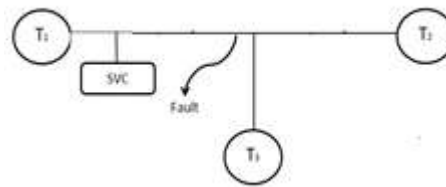


Fig.1 Single line diagram of the three-terminal transmission system compensated with SVC.

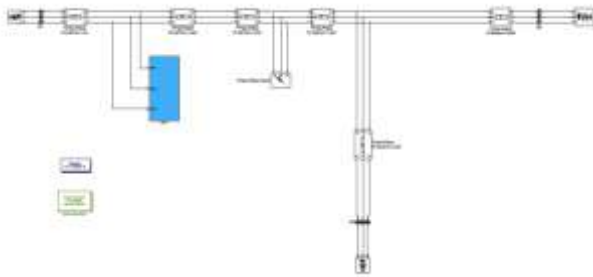


Fig.2 Simulink diagram of the three-terminal transmission system compensated with SVC

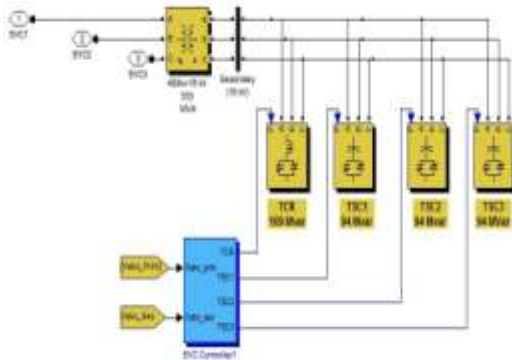


Fig.3 Architecture of the SVC connected in the line.

The scheme has been evaluated using 400KV, 50Hz three terminal transmission system whose line parameters with values  $R_0=0.1888\Omega/\text{km}$ ,  $R_1=0.02\Omega/\text{km}$ ,  $L_0=3.5\text{Mh}/\text{km}$ ,  $L_1=0.94\text{mH}/\text{km}$ ,  $C_0=0.0083\mu\text{f}/\text{km}$ ,  $C_1=0.012\mu\text{f}/\text{km}$ . 16KHZ sampling frequency has been used to capture the high frequency current signals. The system is modeled in Matlab Simulink software for different fault situations. Exhaustive simulations were carried out for L-G, L-L, L-L-G, L-L-L faults at various locations along the same Terminals at which the SVC was connected for compensation and paths taken were Terminal1, Terminal 2, Terminal 3. For each type of fault at a particular location, the fault inception angle was varied to analyse the performance of the proposed scheme. The fault resistance of 5 ohms also being considered. The detail D1 coefficients were used for detection and classification of the type of fault after Synchronized sampling of three phase currents at all terminals were carried out with Bior1.5 mother wavelet to obtain the coefficients ( $D1_1$ ) at terminal 1 over a moving window of half cycle length by analysing the three phase currents of the local terminal. These  $D1_1$  coefficients were further transmitted to the remote end. The detailed coefficients received from the remote end at bus2 ( $D1_2$ ) that were subtracted from the local coefficients ( $D1_1$ ) to obtain effective D1 coefficients ( $D1_E$ ). The Fault Index ( $I_{f1}$ ) of each phase is calculated from the expression  $I_{f1} = \sum |D1_E|$ . The performance of the scheme in detecting and classifying the faults i.e. line(L)-to -ground, line-to-line(L),line-line-to-

ground(L-L-G), triple-line-to-ground(LLL-G) has been evaluated. In all the cases, the theory was able to detect the faults. The fault inception angle was varied from  $20^\circ$  to  $180^\circ$  for all kinds of faults. The simulations show that the fault inception angle has a considerable effect on the phase current samples and Wavelet Transform output of post-fault signals over a moving window of half cycle length.

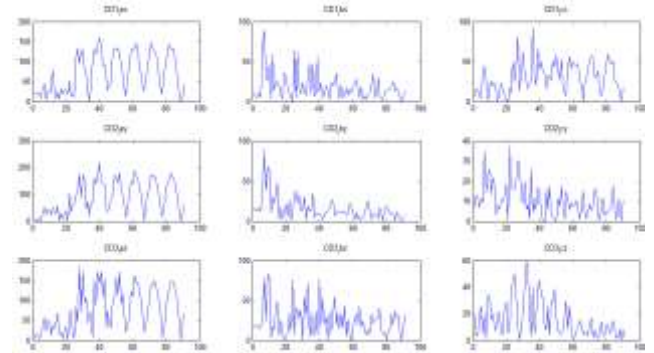


Fig.4 Three Phase waveforms at terminals-1,2,3 for A-G fault occurring at Terminal-1

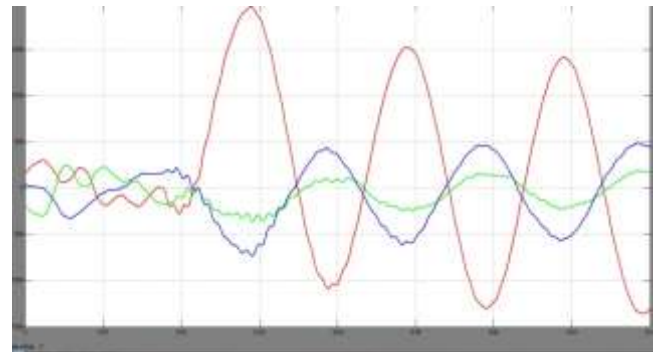


Fig.5 Three Phase waveforms at terminal-1 for A-G Fault at Terminal-1

### 3.1 Fault Detection and classification

#### 3.1.1 Variation of Fault Indices with Fault Inception Angle at a constant Distance of 50km from Terminal-1

##### 3.1.1 A-G Fault



FIA(Degrees)	la	lb	lc	Th
20	1271.833217	79.20743	128.8114	400
40	987.1075048	90.00913	110.6482	400
60	811.3573452	72.45188	159.9909	400
80	820.0404998	50.40479	187.4025	400
100	992.6730704	51.0809	176.7791	400
120	1162.855299	59.83384	156.0886	400
140	989.4574848	53.91198	98.18963	400
160	821.4734904	55.21848	119.923	400
180	810.6653859	49.79	181.4787	400

Table-1 Variation of fault indices with Fault inception angle at a constant distance of 50km from terminal-1 for A-G fault

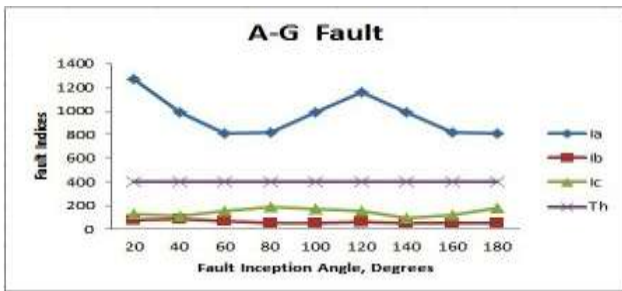


Fig.6 Variation of three phase indices with fault inception angle for A-G fault

### 3.1.2 A-B Fault

FIA(Degrees)	la	lb	lc	Th
20	973.4502	903.8706	166.9134	400
40	802.2101	712.6145	181.8241	400
60	735.1862	726.9879	110.9237	400
80	889.8163	819.6446	125.2801	400
100	1089.165	953.6804	145.9471	400
120	942.0154	843.3124	147.3894	400
140	814.9419	662.5071	190.6312	400
160	777.7515	661.864	177.2188	400
180	884.2833	822.1932	164.5454	400

Table-2 Variation of fault indices with Fault inception angle at a constant distance of 50km from terminal-1 for A-B fault

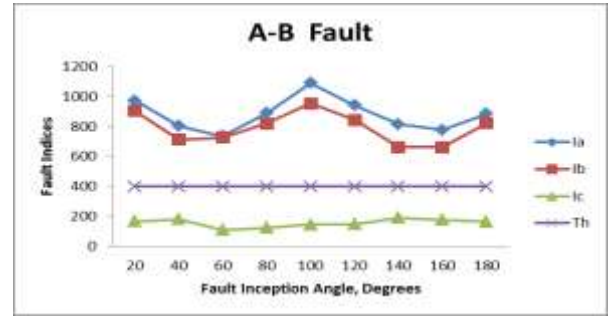


Fig.7 Variation of three phase indices with fault inception angle for A-B fault

### 3.1.3 A-B-G Fault

FIA(Degrees)	la	lb	lc	Th
20	1303.267	866.4209	119.1036	400
40	1008.319	808.551	109.8291	400
60	833.9442	929.9827	95.53111	400
80	852.9438	1136.398	132.0153	400
100	1024.402	1029.217	151.0567	400
120	1190.669	838.5185	161.6527	400
140	999.2071	793.8751	151.7896	400
160	833.143	921.0011	98.88432	400
180	834.3139	1188.036	152.7625	400

Table-3 Variation of fault indices with Fault inception angle at a constant distance of 50km from terminal-1 for A-B-G fault



Fig.8 Variation of three phase indices with fault inception angle for A-B-G fault

### 3.1.4 A-B-C Fault

FIA(Degrees)	la	lb	lc	Th
20	1316.55	884.2554	958.8541	400
40	1034.864	836.6825	1219.739	400
60	854.5136	963.205	1173.001	400
80	855.3133	1174.378	927.3041	400



100	1025.224	1051.634	828.9611	400
120	1201.765	859.6931	904.0615	400
40	1019.61	821.2321	1135.735	400
160	845.4015	958.2384	1256.558	400
180	834.298	1235.035	1024.588	400

Table-4 Variation of fault indices with Fault inception angle at a constant distance of 50km from terminal-1 for A-B-C fault

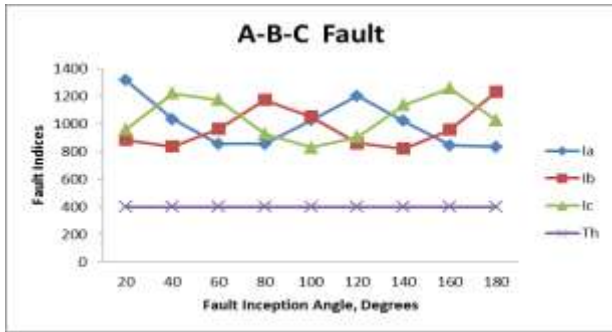


Fig.9 Variation of three phase indices with fault inception angle for A-B-C fault

### 3.2 Variation of Fault Indices with Distance at constant Fault Inception Angle of 100° from Terminal-1

#### 3.2.1 A-G Fault

Table-5 Variation of fault indices with distance at a constant Fault inception angle 100° from terminal-1 for A-G fault

Distance,km	Ia	Ib	Ic	Th
10	1051.316	63.60791	171.2912	400
20	1034.611	76.92684	160.644	400
30	1021.882	65.81182	158.2972	400
40	999.1788	53.20197	183.1805	400
50	992.6731	51.0809	176.7791	400
60	979.4254	55.98399	181.1416	400
70	965.5856	52.05695	198.2961	400
80	948.6568	71.8082	215.2278	400
90	922.269	65.93465	218.1672	400
100	946.7976	84.77081	215.5236	400

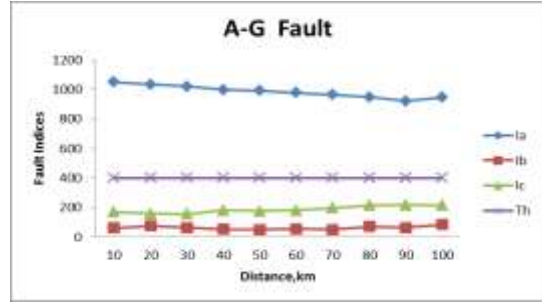


Fig.10 Variation of fault indices with distance at a constant Fault inception angle 100° from terminal-1 for A-G fault

#### 3.2.2 A-B Fault

Table-6 Variation of fault indices with distance at a constant Fault inception angle 100° from terminal-1 for A-B fault

Distance,km	Ia	Ib	Ic	Th
10	1124.623	991.8901	134.6353	400
20	1114.599	982.8986	134.6754	400
30	1105.367	973.6085	135.3096	400
40	1097.163	964.2273	139.5222	400
50	1089.165	953.6804	145.9471	400
60	1081.289	943.3379	150.6737	400
70	1074.627	932.9933	154.0818	400
80	1066.369	925.5402	151.3716	400
90	1058.33	917.5316	150.5474	400
100	1049.015	908.5301	150.259	400

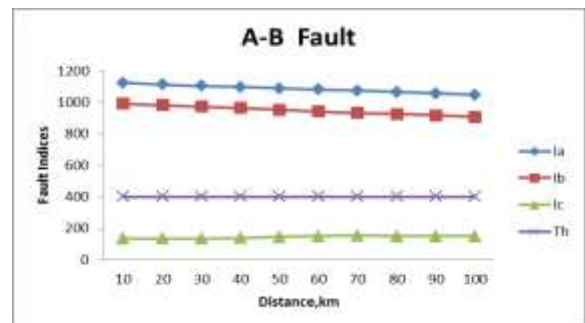


Fig.11 Variation of fault indices with distance at a constant Fault inception angle 100° from terminal-1 for A-B fault

#### 3.2.3 A-B-G Fault



Distance,km	Ia	Ib	Ic	Th
10	1058.031	1083.587	153.7912	400
20	1048.307	1071.315	114.6414	400
30	1028.452	1065.709	116.2819	400
40	1028.587	1046.742	134.9876	400
50	1024.402	1029.217	151.0567	400
60	1021.713	1024.378	157.9488	400
70	1003.567	1017.243	178.6091	400
80	1009.112	1012.804	198.5697	400
90	994.9441	982.4301	235.2386	400
100	1050.825	909.2335	202.3908	400

Table-7 Variation of fault indices with distance at a constant Fault inception angle  $100^{\circ}$  from terminal-1 for A-B-G fault

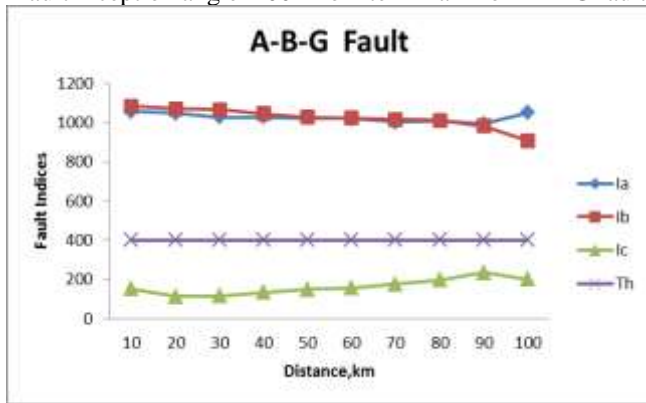


Fig.12 Variation of fault indices with distance at a constant Fault inception angle  $100^{\circ}$  from terminal-1 for A-B-G fault

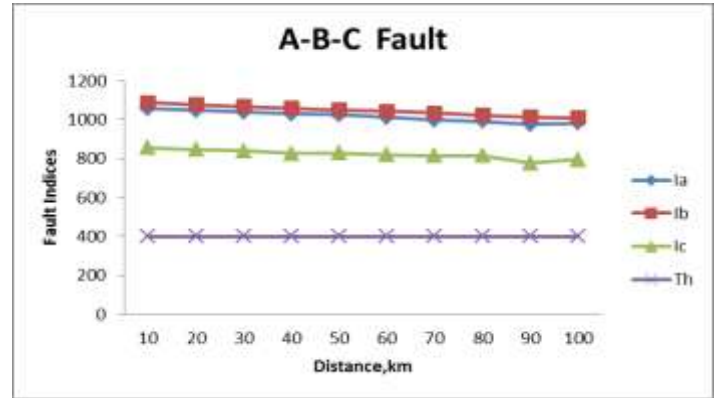


Fig.13 Variation of fault indices with distance at a constant Fault inception angle  $100^{\circ}$  from terminal-1 for A-B-C fault

#### IV. FAULTY TERMINAL IDENTIFICATION

##### 4.1 Variation of Fault Indices with Fault Inception Angle at a constant Distance of 50km from Terminal-1

##### 4.1.1 A-G Fault

FIA(Degrees)	Ia at T1	Ia at T2	Ia at T3
20	1271.833	726.8051	683.8577
40	987.1075	627.0287	636.4459
60	811.3573	525.3702	511.0972
80	820.0405	521.051	476.4155
100	992.6731	616.0908	545.59
120	1162.855	663.8715	588.0599
40	989.4575	596.8371	595.1165
160	821.4735	487.9997	477.6104
180	810.6654	500.8588	462.4231

Table-9 Variation of fault indices with Fault inception angle at a constant distance of 50km from terminal-1 for A-G fault

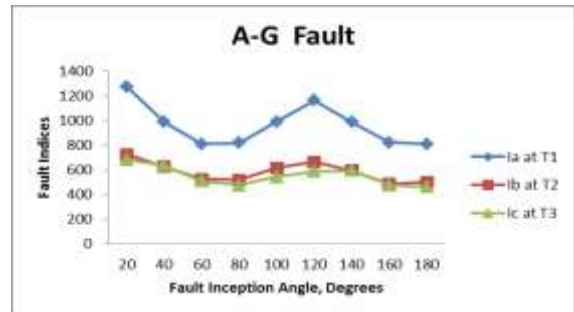


Fig.14 Variation of Fault Indices of phase A at all three terminals with Fault Inception Angle at a constant Distance of 50km from Terminal-1 for A-G fault at terminal-1

### 3.2.4 A-B-C Fault

Table-8 Variation of fault indices with distance at a constant Fault inception angle  $100^{\circ}$  from terminal-1 for A-B-C fault

Distance,km	Ia	Ib	Ic	Th
10	1057.095	1088.119	856.6351	400
20	1047.544	1078.738	848.5567	400
30	1038.983	1069.571	840.6994	400
40	1031.381	1059.667	827.3294	400
50	1025.224	1051.634	828.9611	400
60	1011.849	1043.254	821.4733	400
70	999.57	1034.101	817.0673	400
80	992.7669	1023.726	815.1306	400
90	977.3563	1014.655	777.2148	400
100	983.9326	1010.421	796.1047	400



4.1.2 A-B Fault

FIA(Degrees)	lab at T1	lab at T2	lab at T3
20	938.6604	666.3946	703.6342
40	757.4123	521.0071	542.8018
60	731.0871	483.8972	485.3146
80	854.7305	570.1135	552.9263
100	1021.423	699.6817	678.6525
120	892.6639	637.4908	655.8882
40	738.7245	516.7205	528.0542
160	719.8078	468.2257	460.3936
180	853.2383	570.785	542.8236

Table-10 Variation of fault indices with Fault inception angle at a constant distance of 50km from terminal-1 for A-B fault

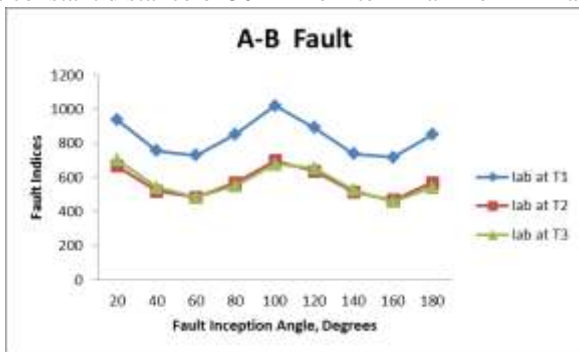


Fig.15 Variation of **Fault Indices of phases A ,B** with **Fault Inception Angle** at a constant **Distance of 50km** from Terminal-1 for A-B fault at terminal-1

4.1.3 A-B-G Fault

FIA(Degrees)	lab at T1	lab at T2	lab at T3
20	1084.844	707.0363	714.2358
40	908.4351	578.3372	579.1884
60	881.9635	545.9187	526.3928
80	994.6709	610.2895	583.5802
100	1026.81	715.6167	703.6842
120	1014.594	662.4321	660.0773
40	896.5411	565.3722	563.0696
160	877.0721	526.2385	504.7701
180	1011.175	605.6401	564.0422

Table-11 Variation of fault indices with Fault inception angle at a constant distance of 50km from terminal-1 for A-B-G fault

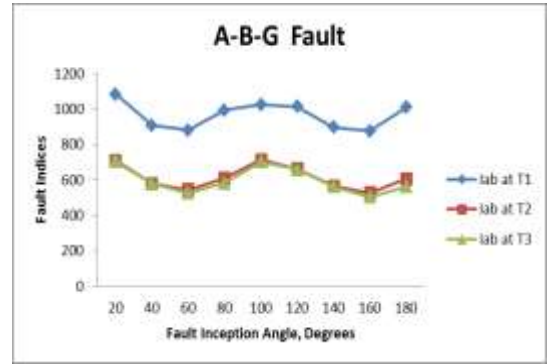


Fig.16 Variation of **Fault Indices of phases A,B** at **all terminals** with **Fault Inception Angle** at a constant **Distance of 50km** from Terminal-1 for A-B-G fault at terminal-1

4.1.4 A-B-C Fault

FIA(Degrees)	lab at T1	lab at T2	lab at T3
20	1053.22	773.2709	766.0341
40	1030.429	717.0384	714.0753
60	996.9065	728.5648	730.2039
80	985.6652	674.7443	672.9073
100	968.6065	693.1663	695.9736
120	988.5065	686.4473	686.1975
40	992.1924	658.7338	663.1065
160	1020.066	732.5465	729.6865
180	1031.307	686.1928	670.6988

Table-12 Variation of fault indices with Fault inception angle at a constant distance of 50km from terminal-1 for A-B-C fault

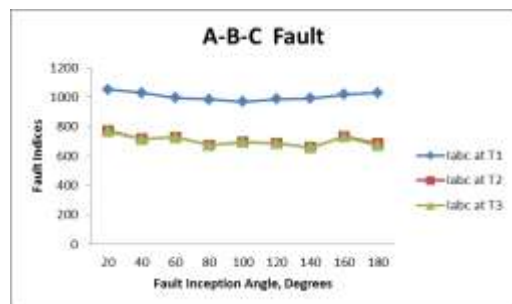


Fig.17. Variation of **Fault Indices of all the three phases** at **all three terminals** with **Fault Inception Angle** at a constant **Distance of 50km** from Terminal-1 for A-B-C fault



**4.2 Variation of Fault Indices with Distance at constant Fault Inception Angle of 100° from Terminal-1**

**4.2.1 A-G Fault**

Distance,km	lab at T1	lab at T2	lab at T3
10	1058.257	649.9823	628.953
20	1048.749	666.6889	645.6596
30	1039.488	684.3381	663.3089
40	1030.695	696.0962	675.0669
50	1021.423	699.6817	678.6525
60	1012.313	701.8885	680.8592
70	1003.81	713.9732	692.9439
80	995.9545	729.4397	708.4104
90	987.9308	737.7481	716.7189
100	978.7725	743.0085	721.9792

Table-13 Variation of fault indices with distance at a constant Fault inception angle of 100° for A-G fault at terminal-1

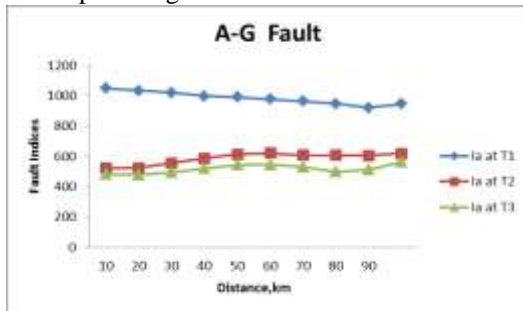


Fig.18 Variation of fault indices with distance at a constant Fault inception angle of 100° for A-G fault at terminal-1

**4.2.2 A-B Fault**

Distance,km	la at T1	la at T2	la at T3
10	1051.316	523.1617	481.7494
20	1034.611	525.8426	479.5232
30	1021.882	555.9562	495.151
40	999.1788	589.0699	523.2
50	992.6731	616.0908	545.59
60	979.4254	621.2073	548.6223
70	965.5856	607.6061	531.4379
80	948.6568	607.9236	500.3229
90	922.269	606.1666	513.2367
100	946.7976	619.3454	562.9958

Table-14 Variation of fault indices with distance at a constant Fault inception angle of 100° for A-B fault at terminal-1

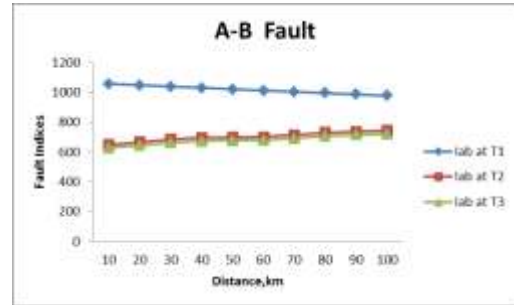


Fig.19 Variation of fault indices with distance at a constant Fault inception angle of 100° for A-B fault at terminal-1

**4.2.3 A-B-G Fault**

FIA(Degrees)	labc at T1	labc at T2	labc at T3
20	1053.22	773.2709	766.0341
40	1030.429	717.0384	714.0753
60	996.9065	728.5648	730.2039
80	985.6652	674.7443	672.9073
100	968.6065	693.1663	695.9736
120	988.5065	686.4473	686.1975
40	992.1924	658.7338	663.1065
160	1020.066	732.5465	729.6865
180	1031.307	686.1928	670.6988

Table-15 Variation of fault indices with distance at a constant Fault inception angle of 100° for A-B-G fault at terminal-1

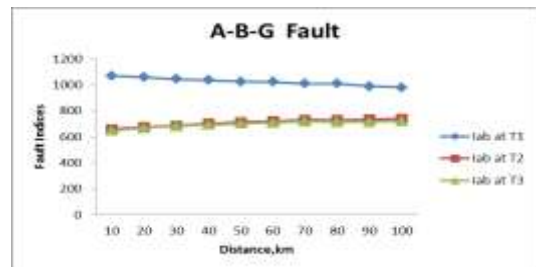


Fig.20 Variation of fault indices with distance at a constant Fault inception angle of 100° for A-B-G fault at terminal-1





#### 4.2.4 A-B-C Fault

Distance,km	labc at T1	labc at T2	labc at T3
10	1000.616	707.6665	672.883
20	991.6129	720.5502	676.2838
30	983.0847	736.5692	682.2419
40	972.7925	740.3053	700.094
50	968.6065	738.1129	695.9736
60	958.859	741.0192	681.3375
70	950.2461	751.7695	678.243
80	943.8744	753.9598	695.0711
90	923.0755	746.5805	680.9352
100	930.1527	769.4886	699.4228

Table-16 Variation of fault indices with distance at a constant Fault inception angle of  $100^0$  for A-B-C fault at terminal-1

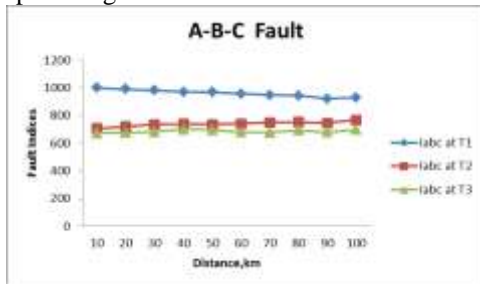


Fig.21 Variation of fault indices with distance at a constant Fault inception angle of  $100^0$  for A-B-C fault at terminal-1

Figures 6-9 indicate the variation of the fault indices with fault inception angle for A-G, A-B, A-B-G, A-B-C faults occurring at a distance of 50km from terminal-1 and Figures 10-13 indicate the variation of fault indices with distance at a fault inception angle of  $100^0$  where the faulty phases have been detected by comparing the fault indices of all the three phase currents with threshold value in which the values of indices of faulty phase(s) was(were) higher than that of the threshold value and that of the healthy phase(s) was(were) lesser than that of threshold value which clearly discriminates the faulty phases from healthy phases.

Tables 1-4 indicate variation of the fault indices of all the three phase currents with fault inception angle for A-G, A-B, A-B-G, A-B-C faults occurring at a distance of 50km from terminal-1 respectively.

Tables 5-8 indicate variation of the fault indices of all the three phase currents with distance at a fault inception angle  $100^0$  for A-G, A-B, A-B-G, A-B-C faults from terminal-1 respectively. Figures 14-17 indicate the variation of the fault indices with fault inception angle at a constant distance of the same phase(s) at all the three terminals for A-G, A-B, A-B-G, A-B-C faults from terminal-1 where the comparison of the

indices identifies the faulty terminal where the indices at the faulty terminal for the particular phase(s) were higher than that of the indices at the remaining terminals which clearly identifies the faulty terminal. Figures 18-21 indicate the variation of the fault indices with distance at a constant fault inception angle of the same phase(s) at all the three terminals for A-G, A-B, A-B-G, A-B-C faults from terminal-1 where the comparison of the indices identifies the faulty terminal where the indices at the faulty terminal for the particular phase(s) were higher than that of the indices at the remaining terminals which clearly identifies the faulty terminal.

Tables 9-12 indicate the variation of the fault indices of the same phase(s) at all terminals with fault inception angle at a distance of 50km from terminal-1 for A-G, A-B, A-B-G, A-B-C faults occurring at terminal-1 respectively. Tables 13-16 indicate the variation of the fault indices of the same phase(s) at all terminals with distance at a fault inception angle of  $100^0$  from terminal-1 for A-G, A-B, A-B-G, A-B-C faults occurring at terminal-1 respectively.

#### V. FAULT LOCATION ESTIMATION USING FUZZY INFERENCE SYSTEM

After the fault detection, classification and faulty terminal identification, the fault location has been estimated with Fuzzy logic. For this purpose, the three phase current signals at the corresponding terminal have been decomposed with Bior 1.5 mother wavelet and the fault indices obtained were the inputs to the Fuzzy Inference System. The standard fuzzy membership function taken was triangular and the output function taken was distance(D). Each input variable is quantized into the linguistic variables such as very low(VL), Low(L), high(H), very high(VH) for the universe of discourse spanning from 0 to 1 and for the output variable, it is the length of the transmission system divided into four zones D1,D2,D3,D4. The inputs are combined together based on the expert opinion and the possible rules are framed and the output is defuzzified to get the crisp value of D. Simulations were carried out considering variations in fault location and fault inception angle for different types of faults.

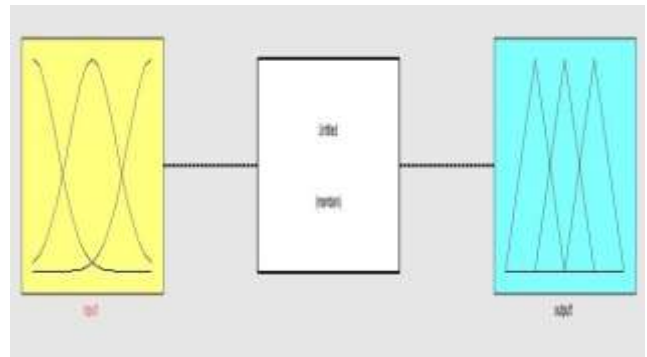


Fig.22 Fuzzy Inference System for fault location estimation

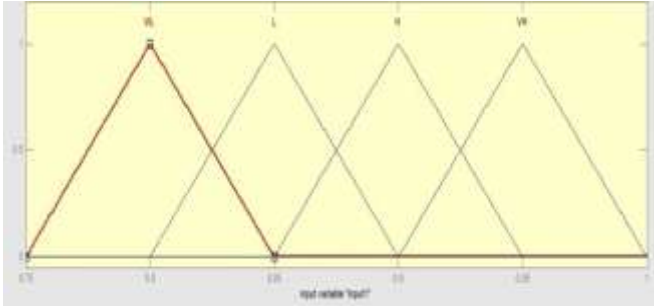


Figure 23: Input variable (fault indices) for fault location from terminal-1

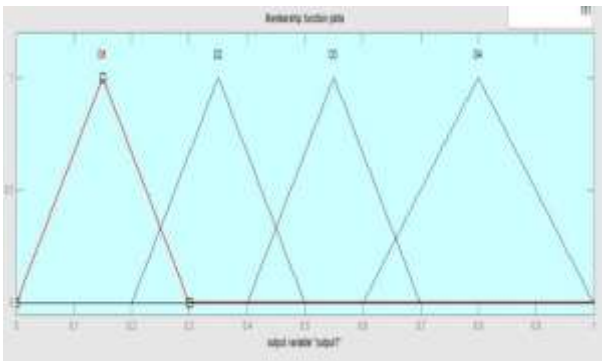


Fig 24: Output variable (distance) for location estimation from terminal-1.

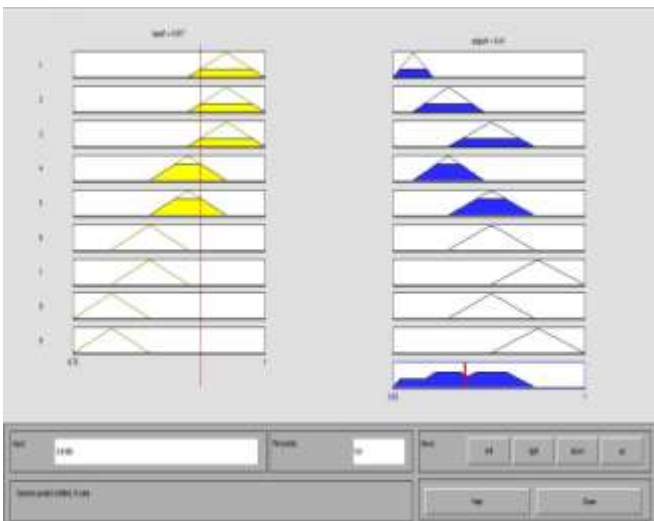


Fig.25 Fuzzy rule base

Fault type	Actual distance from terminal-1 (KM)	Transmission system	
		Fuzzy distance, (KM)	Error distance
A-G	20	17.3	2.7
	50	42.8	7.2
A-B	20	15.2	4.8
	50	43.14	6.86
A-B-G	20	16.4	3.6
	50	43.7	7.3
A-B-C	20	16.6	3.4
	50	46.5	3.5

Table-17 Fault location estimation

### VI. CONCLUSION

A wavelet-fuzzy approach for the protection of three terminal transmission line under the faults occurring on the SVC compensated line has been presented in this work. A fault detection scheme based on the discrete approximation of the Bior 1.5 wavelet has been proposed. An abrupt change of current component when a fault occurs on the system can be clearly detected by the analysis of decomposing the current waveform and comparing with the threshold value to detect and classify the faulty phases. This method also successfully classifies the faulty terminal under the varying conditions like fault distance, fault inception angle, fault impedance and proved to be effective in all the conditions for all types of faults occurring at all the terminals and also the fault location estimation for all distances with minimum error by utilizing fuzzy inference system which was found to be an effective tool. The simulation studies demonstrate that the proposed algorithm is effective in the protection of the transmission lines.



## VII. REFERENCES

- [1].Bo,Z.Q.; "A new non-communication protection technique for transmission lines," IEEE Transactions on Power Delivery, 1998, 13, (4), pp. 1073-1078
- [2].Bhalija, B., and Maheswari, R.P, "High resistance faults on two terminal parallel transmission line; analysis, simulation studies, and an adaptive distance relaying scheme", IEEE Transactions on Power Delivery., 2007, 22, (2), pp. 801-812
- [3].Brahma, S.M and Girgis, A.A. "Fault location on a transmission line using synchronized voltage measurements," IEEE Transactions on Power Delivery, 2004,9,(4),pp.1619-1622.
- [4].Lyonette, D.R.M., Bo,Z.Q., Weller, G., and Jiang,G, "A new directional comparison technique for the protection of teed transmission circuits". Power Engineering Society, Winter Meeting, IEEE., January 2000, vol.3, pp. 1979-1984
- [5] Bhalija,B.,and Maheswari, R.P; "New differential protection scheme for tapped transmission line". IET Generation, Transmission. Distribution., 2008 , 2,(2) ,pp. 271-279
- [6] Al-Fakhri,B , "The theory and application of differential protection of multi-terminal lines without synchronization using vector difference as restraint quantity-simulation study." 8<sup>th</sup> IEEE International Conference,DPSP, April 2004, Vol.2, pp. 404-409.
- [7].T.Funabashi, H.Otoguro, Y.Mizuma, L.Dube, and A.Ametani, "Digital fault location algorithm for parallel double- circuit multi terminal transmission lines." IEEE Transactions on Power Delivery, vol.15. 2, pp. 531-537 April-2000
- [8].Prarthana Warlyani, Anamika Jain,A.S.Thoke, R.N.Patel., "Fault classification and faulty section identification in Teed transmission circuits using ANN". International Journal of Computer and Electrical Engineering , Vol.3,No.6 Dec-2012
- [9].Peyman Jafarian, Majid Sanaye-Pasand "High-frequency transients-based protection of multi-terminal transmission lines using the SVM technique." IEEE, 0885-8977,2012
- [10]A.H.Osman ,O.P Malik "Wavelet transform approach to distance protection of transmission lines",IEEE Transactions on Power Delivery,. October 2001.
- [11].K.Saravanababu,P.Balakrishnan,K.Sathiyasekhar "Transmission line fault detection, classification and location using DWT". International conference on Power, Energy, and Control, ICPEC, 6-8<sup>th</sup> Feb-2013
- [12].Atthapol Ngaoppitakkal et al, "Identifying types of simultaneous faults in transmission line using DWT and Fuzzy logic algorithm." International Journal of Innovative Computing, Information and Control, Vol-7 July 2013.
- [13]Chul-Hwan Kim, Hyun Kim, Young-Hum Ko, Sung-Hyun Byun, Raj.K. Aggarwal, Allan T.Johny "A novel fault-detection techniques of high impedance arcing faults (HIF) in transmission lines using the wavelet transform" IEEE Transactions on Power Delivery. October 2002
- [14].M.Kowsalya,K.K.Ray, D.P.Kothari,"positioning of SVC and STATCOM in a long transmission line." International journal of recent trends in engineering, vol.2, No.5, Nov.(2009)
- [15].F.A.Albasri, T.S.Sidhu, R.K.Varma, "Impact of shunt FACTS on distance protection of transmission lines", IEEE transactions on power delivery, vol.18, No.1, pp.34-42January-(2003).
- [16].Rekha, Manmohankumar, A.K.Singh, "Fuzzy controlled SVC for reactive power control of long transmission lines" Iranian journal of of science and technology , Transactions in electrical engineering, Vol.4,No.7, pp.15-22 (2014).
- [17]S.A.Hosseini,H.Askarian,Abyaneni,S.H.H.Sadeghi,Razavi,M.Karami, "Presenting a new method for identifying Fault location in microgrids using harmonic impedance" International journal of science and technology, Transactions of electrical engineering, Vol.39, No.E2, pp.167-182, (2015).
- [18] Feng Liang, B.Jeyasurya, "Transmission line distance protection using wavelet transform algorithm," IEEE transactions on power delivery, Vol.19,No.2 April,(2004).
- [19].G.Ravikumar, Sk.AbdulGafoor, S.S.Tulasiram, "Fuzzy-Wavelet based double transmission line protection in the presence of SVC", Journal of the Institution of Engineers(India), Springer,July(2014).